Early Himalayan exhumation: Isotopic constraints from the Indian foreland basin

Yani Najman†,‡, Mike Bickle*,† and Hazel Chapman†

†Department of Earth Sciences, Cambridge University, Downing St., Cambridge CB2 3EQ, UK, ‡Department of Geology & Geophysics, Edinburgh University, West Mains Road, Edinburgh EH9 3JW, UK

ABSTRACT

Nd- and Sr-isotopic compositions of Palaeogene foreland basin sediments are used to provide insights into early Himalayan evolution, particularly the timing of exposure of high $^{87}Sr/^{86}Sr$ units, erosion of which may have caused the late Tertiary increase in oceanic Sr-isotopic ratios. During the late Palaeocene–early Eocene, erosion was from mixed sources including suture zone rocks. Exhumation of the High Himalaya was occurring by the time of deposition of alluvial sediments after mid-Oligocene times and this source has dominated Himalayan sediments from at least this time until the present day. The transition is interpreted to reflect exhumation of 'basement rocks' of the Indian plate, when the High Himalaya became a sufficient topographic barrier to separate suture zone rocks from the foreland basin. The marked rise in seawater $^{87}Sr/^{86}Sr$ from 40 Ma is consistent with the erosion of a Himalayan source with a high $^{87}Sr/^{86}Sr$ ratio.

Terra Nova, 12, 28–34, 2000

Introduction

The Himalayas are the prime example of an active collisional orogen. Their kinematics form the basis of our understanding of crustal deformation processes in collisional zones (e.g. England and McKenzie, 1982; Tapponnier *et al*., 1982; Houseman and England, 1993). The associated uplift and erosion may moderate long-term changes in global climate (e.g. Raymo, 1991). A critical limit to our understanding of the evolution of mountain belts is that observations on their kinematics are only possible at the present day. Past kinematics, responsible for today's crustal expression, must be inferred from the geological record. In this paper we use the Sr and Nd isotopic composition of Himalayan-derived sediments, deposited in the foreland basin, to map the history of exhumation and erosion of various isotopically distinct crustal units. Our results put further constraints on the timing of erosion of the $^{87}Sr/^{86}Sr$ enriched rocks, which may have had a significant influence on the rise in seawater $^{87}Sr/^{86}Sr$ since ~40 Ma (Hodell *et al*., 1990; Richter *et al*., 1992).

Geological setting

Himalayan tectonics

Southwards directed and propagating thrusting has constructed the Himalayan chain from six main tectonic units (Fig. 1) (listed from north to south below).

1 The Trans-Himalayan zone, the Andean-type northern margin of Tethys formed by Cretaceous to Eocene calc-alkaline plutons intruding the Eurasian continental crust (Honegger *et al*., 1982; Le Fort, 1996);

2 The Indus–Tsangpo Suture Zone, comprising deep-water Indian continental rise sediments, ophiolite-bearing accretionary complexes, island arc volcanics and fore-arc basin sediments, as well as post-early Eocene molasse-type sediments (e.g. Garzanti and Van Haver, 1988; Robertson and Degnan, 1993);

3 The Tibetan Sedimentary Series, deposited on the continental margin of the Indian plate consisting of mixed clastics and carbonates in the late Precambrian to early Permian and mainly shelf carbonate in the late Permian to early Eocene, unconformably overlain by the Chulung La collisional deposits (Critelli and Garzanti, 1994; Searle *et al*., 1997a). The Tibetan Sedimentary Series is now juxtaposed against the High Himalayan Crystalline Series to the south by normal faulting on the South Tibetan Detachment Zone.

4 The High Himalayan Crystalline Series is derived from late Proterozoic and younger Indian continental crust which underwent high-grade regional metamorphism and intrusion by leucogranites during Himalayan orogenesis (e.g. Le Fort *et al*., 1987; Parrish and Hodges, 1996). This unit is emplaced over the Lesser Himalayan Series to the south by the Main Central Thrust (MCT).

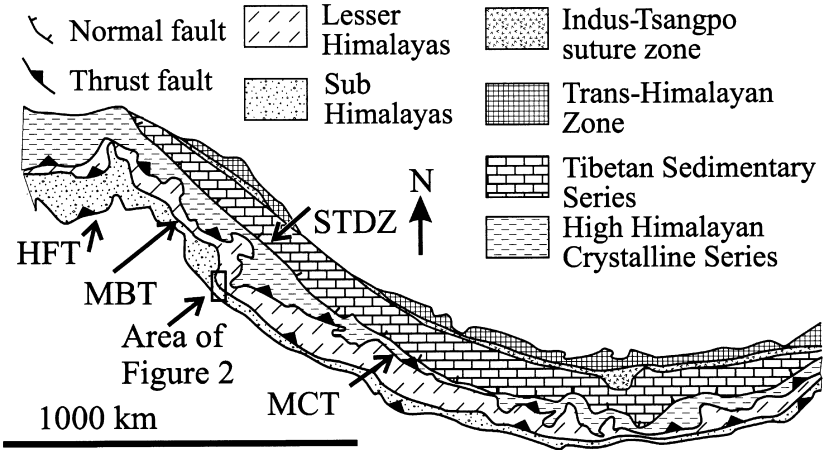

Fig. 1 Himalayan orogenic belt showing potential Himalayan source rocks for the sediments of the foredeep. Study area boxed. MCT, Main Central Thrust; STDZ, South Tibetan Detachment Zone; MBT, Main Boundary Thrust; HFT = MFT, Main Frontal Thrust.

*Correspondence: Tel.: +44/ 1223 333400; Fax: +44/ 1223 333450; E-mail: mb72@esc.cam.ac.uk

5 The Lesser Himalayan Series, a low-grade, mid-Proterozoic clastic and carbonate sequence, probably originally deposited on Indian continental crust (e.g. Valdiya, 1980; Parrish and Hodges, 1996). The Lesser Himalayan Series is emplaced on the sub-Himalayan units by the Main Boundary Thrust.
6 The Sub-Himalaya comprising sediments eroded from the Himalayan orogen and deposited in the peripheral foredeep south of the mountain belt (e.g. Najman *et al.*, 1993; Critelli and Garzanti, 1994; Najman and Garzanti, 2000).

The structural evolution of the Himalayan orogen initiated with continental collision in the latest Palaeocene at ~ 50 Ma (e.g. Le Fort, 1996; Rowley, 1996). Crustal thickening resulting from thrusting of suture zone rocks, the Tibetan Sedimentary Series and the precursors of the High Himalayan Crystalline Series, resulted in Barrovian metamorphism that peaked at 40–30 Ma (Hodges and Silverberg, 1988; Inger and Harris, 1992; Hodges *et al.*, 1994; Vance and Harris, 1999). The High Himalaya were then thrust over the Lesser Himalaya along the MCT, active at ~ 22 Ma (Hubbard and Harrison, 1989; Hodges *et al.*, 1996) with the youngest movement dated at ~ 6 Ma (Harrison *et al.*, 1997). Extensional faulting along the South Tibetan Detachment Zone took place between ~ 23 Ma and ~15 Ma (e.g. Searle *et al.*, 1999). Southerly propagation of the thrust stack continued with the emplacement of the Lesser Himalaya over the Sub Himalaya along the Main Boundary Thrust, active in the middle–late Miocene (e.g. Meigs *et al.*, 1995), and the presently active Main Frontal Thrust to the south which emplaces older units of the Sub-Himalaya on the youngest sediments in the Indo-Gangetic Plain.

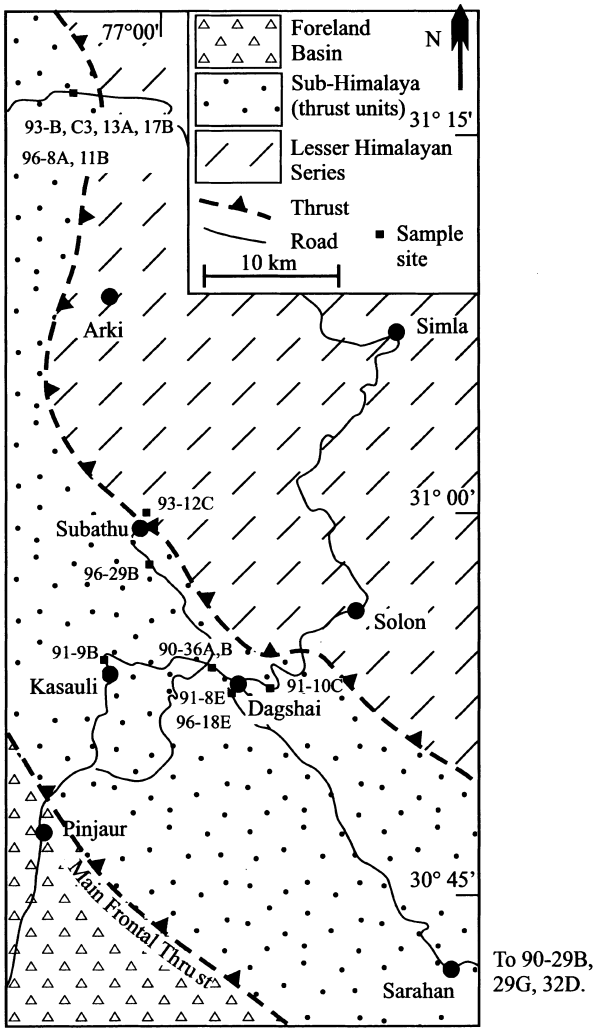

Fig. 2 Sample locations and distribution of major tectonic units (compiled by Najman, 1995). Mapping of distribution of Subathu, Dagshai and Kasauli Formations is restricted mainly to road cuts and river sections.

The foreland basin

Sediments eroded from the Himalayan chain have been deposited in a foreland basin that extends along the entire southern flank of the orogen. We sampled older units of the foreland basin in Himachal Pradesh, where the Sub-Himalaya consists of a series of Tertiary sediment thrust slices beneath the Main Boundary Thrust (Fig. 2). Within these thrust sheets, the sedimentary Subathu, Dagshai, Kasauli and Siwalik Formations (Gansser, 1964; Bhatia, 1982; Fig. 2) are often poorly exposed, largely lacking in fossils, and complexly intercalated. Correlation and identification of these formations is primarily by their lithostratigraphic attributes (Najman *et al.*, 1993).

The Subathu Formation is well dated by a marine fauna between late Palaeocene and lower mid-Eocene (Lower Lutetian) established by Mathur (1980), and consists of limestones, mudstones and very fine-grained sandstones. Detrital material is derived predominantly from pre-existing sedimentary rocks with subordinate mafic igneous input identified by lithic fragments and Cr-spinel (Najman and Garzanti, 2000). Najman *et al.* (1993, 1997) showed that the alluvial Dagshai Formation overlies the Subathu Formation stratigraphically. The Dagshai Formation, consisting of red-coloured mudstones, sandstones and caliche, was dated using palaeomagnetic inclinations at 36 ± 7 Myr age (2 σ) by Najman *et al.* (1994); however, it was dated subsequently to be younger than mid-Oligocene by Najman *et al.* (1997), with ages in the range 25 to 32 Myr using Himalayan detrital muscovite ^{40}Ar–^{39}Ar (single grain, total fusion), and by Najman *et al.* (1999), with fission-track zircon ages of 30 Myr at the base of the succession. Derivation was predominantly from a very low-grade metamorphic source (Najman and Garzanti, 2000). The conformably overlying alluvial Kasauli Formation comprises mainly grey sandstones and subordinate fine-grained material de-

rived from a garnet-grade metamorphic source (Najman and Garzanti, 2000). It is dated by its early to mid-Miocene fossil flora (Fiestmantel, 1882), with Himalayan detrital muscovite Ar–Ar ages mostly between 22 and 32 Myr (Najman *et al.*, 1997), and it is older in age than the overlying alluvial Siwalik Group, magnetostratigraphically dated at 14 Myr old (Johnson *et al.*, 1985; Meigs *et al.*, 1995; Burbank *et al.*, 1996).

Methodology

Foreland basin deposits preserve a well-mixed average of sediment produced by collisional orogenic belts because transport distances are long prior to deposition by the major river in the foreland basin. In the Himalayas antecedant drainage results in the Ganges and its major tributaries crossing all the main Himalayan tectonic units (Friend, 1998) delivering relatively well-mixed sediment prior to further mixing in the foredeep.

Sediment Sm–Nd isotopic systematics provide ideal indicators for source terrains because rare-earth elements are relatively insoluble and fractionation by sedimentary sorting or grain-size variation generally has only limited impact (Taylor and McLennan, 1985). Sr is soluble and shows large differences between minerals that have very different Rb/Sr ratios. Nevertheless, the large difference in $^{87}Sr/^{86}Sr$ between the Himalayan source terrains appear to be reflected in the characteristic $^{87}Sr/^{86}Sr$ of their detrital sediments.

We use both the Nd and Sr isotopic composition of the sediments to distinguish possible sources (Fig. 3a–c). Sample localities are shown on Fig. 2 and Sm–Nd and Rb–Sr isotopic analyses in Table 1. The influence of sedimentary sorting on Sm–Nd isotopic systematics was minimized by sampling very fine-grained to fine-grained sandstones, with medium-grained sandstones used where alternatives were unavailable. Subathu Formation samples contain significant amounts of primary carbonate. Some Dagshai and Kasauli Formation samples contain carbonate cement. Carbonate was removed by leaching with 1 M glacial acetic acid for between 10 minutes and 12 hours. Comparison of leach and residues indicates that the carbonate contained a minor fraction of the Nd, but that

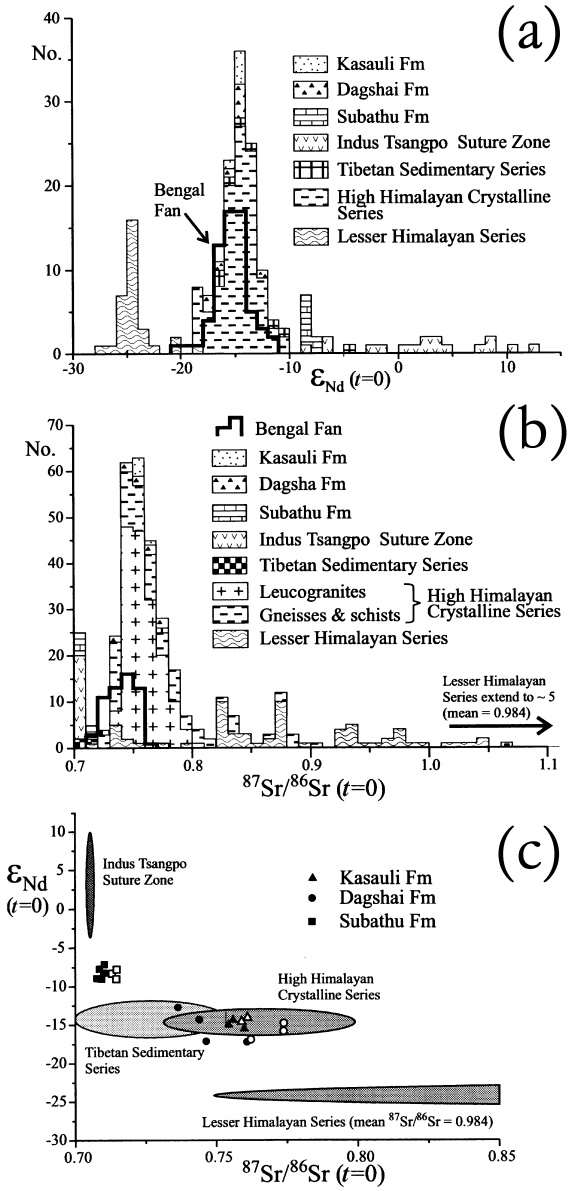

Fig. 3 Isotopic data from the foredeep sediments compared with that from Himalayan units. (a) ε_{Nd} (at zero-age) for foredeep samples compared with data published on main Himalayan units [Vidal *et al.* (1982), Deniel *et al.* (1986, 1987), France-Lanord and Le Fort (1988), Stern *et al.* (1989), Peucat *et al.* (1989), Ferrara *et al.* (1991), France-Lanord *et al.* (1993), Inger and Harris (1993), Massey (1994), Parrish and Hodges (1996), Ayres and Harris (1997), Searle *et al.* (1997b), Harrison *et al.* (1999), Ahmad *et al.* (2000)]. Data from Indus Tsangpo Suture Zone weighted in favour of samples of ophiolite (Ahmad, unpubl. data analysed by procedures given in caption to Table 1). The solid line shows data on mineral separates from Bay of Bengal fan from France-Lanord *et al.* (1993), Derry and France-Lanord (1996) drawn as separate histogram. (b) $^{87}Sr/^{86}Sr$ ratios for leached foredeep samples compared with main Himalayan units. The sources are the same as for Fig. 3a with addition of data from Dietrich and Gansser (1981), Kai (1981) Ferrara *et al.* (1983), Trivedi *et al.* (1984), Scaillet *et al.* (1990) and Searle and Fryer (1986). (c) Nd–Sr isotopic data from foredeep samples compared with Himalayan tectonic units on Nd–Sr isotopic diagram (whole-rock as solid symbols, residues from leaching as open symbols). Ellipses illustrate 1 σ distributions of fields but with $^{87}Sr/^{86}Sr$ ratios > 2 excluded from average Lesser Himalayan Series. Note that leucogranites are over-represented in the High Himalayan Crystalline Series but that their inclusion makes no substantive difference to mean or standard deviation of data. Ophiolites are over-represented in the dataset from the Indus Tsangpo Suture Zone (Ahmad, unpubl. data) and minimum ε_{Nd} values are −8 in this zone.

Table 1 Rb–Sr and Sm–Nd data.

Sample No	analysis type*	grain size†	Rb‡	Sr‡	Rb/Sr	$^{87}Sr/^{86}Sr$	2σ	Sm (ppm)	Nd (ppm)	Sm/Nd	$^{143}Nd/^{144}Nd$	2σ	ε_{Nd} (t=0)§	Co-ordinates π North	Co-ordinates π East
Subathu Formation															
90-32D	wr	v.f-g	10.3	335.3	0.031	0.709993	16	3.21	13.34	0.2407	0.512209	8	−8.4	29° 52′	78° 32′
90-36A	wr	v.f-g	25.3	213.3	0.119	0.708962	18	4.38	20.18	0.2172	0.512190	10	−8.7	30° 53.96′	77° 1.66′
90-36B	wr	v.f-g	22.2	148.0	0.15	0.709168	12	4.38	20.07	0.2184	0.512236	10	−7.8	30° 53.96′	77° 1.66′
	res		40.8	55.3	0.738	0.712885	14	5.28	24.55	0.2152	0.512214	9	−8.3		
	L(10)		1.15%	80.1%	0.002	0.708209	10								
93-12C	wr	v.f-g	27.1	180.8	0.15	0.709682	18	4.59	19.54	0.2348	0.512236	5	−7.8	30° 58.44′	76° 58.76′
	res		37.2	45.3	0.822	0.713238	14	3.51	18.99	0.1847	0.512213	10	−8.3		
	L(10)		1.23%	82.8%	0.002	0.708936	12								
93-13A	wr	v.f-g	43.2	342.4	0.126	0.709597	18	4.93	23.57	0.2093	0.512206	6	−8.4	31° 14.48′	76° 54.80′
	res		69.7	66.6	1.048	0.714507	18	5.16	27.78	0.1850	0.512179	17	−9.0		
	L(10)		0.76%	8.3%	0.001	0.708899	12								
Basal Dagshai Formation															
93-B	wr	m-g	69.5	30.2	2.302	0.754075	10	5.65	29.05	0.1944	0.511890	11	−14.6	31° 15.59′	76° 54.82′
93-C3	wr	f-g	65.8	27.1	2.429	0.752872	16	4.64	23.21	0.2000	0.511870	7	−15.0	31° 15.01′	76° 54.87′
Dagshai Formation															
90-29G	wr	f-g	63.0	45.2	1.392	0.743998	18	6.28	34.23	0.1836	0.511906	10	−14.3	30° 32.64′	77° 49.27′
91-8E	wr	m-g	48.2	13.5	3.582	0.760822	22	4.17	21.84	0.1909	0.511758	3	−17.2	30° 53′	77° 03.00′
	res		49.3	13.3	3.698	0.762225	16	3.91	20.84	0.1876	0.511770	10	−16.9		
	L(10)		0.25%	4.5%	0.25	0.722062	24								
96-11B	wr	v.f-g	41.4	17.9	2.316	0.746373	20	2.33	14.22	0.1640	0.511761	15	−17.1	31° 15.09′	76° 54.80′
96-18E	res	v.f-g	111.6	28.0	3.984	0.773757	12	5.76	31.22	0.1843	0.511826	8	−15.8	30° 53.62′	77° 02.15′
	L(10)		0.36%	6.3%	0.182	0.734888	12								
	L (o/n)		0.41%	6.1%	0.231	0.734111	14								
90-29B	wr	f-g	69.6	71.3	0.976	0.736468	16	4.38	23.68	0.1851	0.511988	9	−12.7	30° 32.64′	77° 49.27′
96-29B	res	m-g	71.8	19.4	3.697	0.773854	14	4.70	23.91	0.1964	0.511880	9	−14.8	30° 57.83′	76° 59.49′
	L(10)		0.48%	6.9%	0.273	0.740510	18								
Kasauli Formation															
91-9B	wr	m-g	86.7	61.6	1.412	0.755880	12	5.62	29.03	0.1934	0.511901	3	−14.4	30° 54.11′	76° 57.64′
	res		78.5	49.2	1.596	0.758922	12	5.08	26.45	0.1922	0.511889	9	−14.6		
	L(10)		0.43%	17.2%	0.033	0.740169	10								
	L (o/n)		0.59%	17.7%	0.048	0.740421	10								
91-10C	wr	m-g	85.4	33.6	2.543	0.759927	20	5.86	29.46	0.1989	0.511842	3	−15.5	30° 53.5′	77° 03.5′
93-17B	wr	m-g	73.4	52.6	1.394	0.754310	18	6.23	32.11	0.1939	0.511869	6	−15.0		
96-8A	res	v.f-g	77.0	31.3	2.456	0.761054	14	3.35	16.22	0.2066	0.511916	7	−14.1	31° 15.32′	76° 51.52′
	L(10)		0.90%	73.9%	0.008	0.739480	12								

*wr = unleached whole-rock, L(10) = 10 minute leach in 1 molar acetic acid, L(o/n) = leach overnight in 1 molar acetic acid, res = residue after leaching.
†v.f-g = very fine grained, f-g = fine grained, m-g = medium grained
‡Concentrations in ppm for whole-rock and residue samples, as percent (%) of total Sr in sample for leachates
§ε_{Nd} calculated at time = 0 for CHUR $^{143}Nd/^{144}Nd = 0.512638$
Rb & Sr analyses by isotope dilution using mixed ^{87}Rb–^{84}Sr spike (Bickle *et al.*, 1988), $^{87}Sr/^{86}Sr$, Sm, Nd and $^{143}Nd/^{144}Nd$ analysed as by Ahmad *et al.* (2000), Sm/Nd ratios accurate to ±0.2% (1σ), concentrations to ±5%, $^{143}Nd/^{144}Nd$ normalised to $^{146}Nd/^{144}Nd = 0.7219$. Errors fractional.
Total Sm blanks <200 pg, Nd blanks <1 ng, Sr blanks <1 ng, and Rb blanks <100 pg for rock dissolutions.
πCoordinates from GPS readings except those quoted to two figures interpolated from base map.

leach and residue $^{87}Sr/^{86}Sr$ ratios are very different.

Nd and Sr isotopic provenance

Figure 3 illustrates Nd and Sr isotopic compositions of four of the major Himalayan tectonic units. The fields on Fig. 3(c) show that the High Himalayan Crystalline Series and Lesser Himalayan Series, the units being eroded most rapidly today, have very different Sm–Nd and Rb–Sr isotopic systematics. The Lesser Himalayan Series is distinct from all the other major units with low ε_{Nd} (~−25) and high $^{87}Sr/^{86}Sr$ values (mostly > 0.8) reflecting derivation from the Archaean rocks of the Indian Craton during the mid-Proterozoic. The High Himalayan Crystalline Series and undersampled Tibetan Sedimentary Series have similar Sm–Nd isotopic compositions (ε_{Nd} ~−15) but different ranges of $^{87}Sr/^{86}Sr$ ratios (Tibetan Sedimentary Series ~ 0.705–0.730, High Himalayan Crystalline Series mostly ~0.730–0.820). High Himalayan leucogranites with high $^{87}Sr/^{86}Sr$ ratios (0.715–0.805) are over-represented in Fig. 3(b). Relatively few sam-

ples are available from the diverse Indus Tsangpo Suture Zone, but their relatively low $^{87}Sr/^{86}Sr$ ratios (< 0.710) and mantle-like ε_{Nd} values (-7 to $+$ 13), are consistent with the abundance of ophiolite and island arc igneous rocks in the unit.

Figure 3 also illustrates the Sr and Nd isotopic composition of the foreland basin samples analysed in this study (Table 1). The Subathu Formation ($\varepsilon_{Nd} \sim$–9, $^{87}Sr/^{86}Sr$ on leached residues $\sim$ 0.710–0.715) plots between the fields occupied by the Tibetan Sedimentary Series and Indus Tsangpo Suture Zone samples (Fig. 3c). By contrast the Dagshai and Kasauli Formation samples have Nd and Sr isotopic compositions ($\varepsilon_{Nd} \sim -12$ to -18, $^{87}Sr/^{86}Sr$ of leached samples $\sim$ 0.755–0.775) characteristic of the High Himalayan Crystalline Series or the highest $^{87}Sr/^{86}Sr$ rocks of the Tibetan Sedimentary Series. These changes in Himalayan source area through time are consistent with the presence of serpentinite clasts and Cr-spinel in Subathu Formation sandstones, where as these occur rarely in the Dagshai and Kasauli Formations (Najman and Garzanti, 2000).

Significant contributions from two additional potential sources, the mainly Archaean Indian Craton ($\varepsilon_{Nd} < -30$; Peucat *et al.*, 1989) and 65 Myr old Deccan Trap flood basalts ($\varepsilon_{Nd} < \sim 0$; Lightfoot *et al.*, 1990) seem unlikely because (i) sources with very low ε_{Nd} values (Indian Craton) do not make a significant contribution to the Himalayan foredeep, (ii) the Dagshai and Kasauli formations do not contain detrital minerals or rock fragments characteristic of Archaean crust; and (iii) the serpentinite clasts and composition of the detrital Cr-spinels in the Subathu Formation imply that its mafic component is ophiolite, not komatiite or flood basalt-derived (Najman and Garzanti, 2000). Drill cores from the Bengal Fan provide a record of sediment shed from the Himalayas from 17 Ma to the present. Nd and Sr isotopic analyses show that throughout this period, the dominant source of sediment to the Bengal fan was the High Himalayan Crystalline Series (Fig. 3; Bouquillon *et al.*, 1990; France-Lanord *et al.*, 1993; Galy *et al.*, 1996). This implies that the High Himalayan Crystalline Series and its early nonmetamorphosed precursors have provided the bulk of the Himalayan erosional detritus from deposition of the Dagshai Formation until the present day.

Comparison with the marine Sr record

The marine Sr-isotopic record exhibits a sudden monotonic increase in $^{87}Sr/^{86}Sr$ ratio from 40 Ma which has been ascribed to initiation of rapid Himalayan uplift and erosion, causing a significant additional flux of high $^{87}Sr/^{86}Sr$ strontium to the oceans (Hodell *et al.*, 1990; Richter *et al.*, 1992). The cause of the atypically high $^{87}Sr/^{86}Sr$ ratio at high Sr concentrations in Himalayan rivers is controversial. Today, Himalayan rivers receive significant contributions of high $^{87}Sr/^{86}Sr$ strontium from silicate and carbonate rocks in both the High Himalayan Crystalline Series and the Lesser Himalayan Series, although the relative contributions from each source are controversial (Harris *et al.*, 1998; Singh *et al.*, 1998; Galy and France-Lanord., 1999).

The 40 Ma inflexion in the seawater Sr-isotope curve occurs in the gap in the sedimentary record between deposition of the youngest low $^{87}Sr/^{86}Sr$ Subathu Formation rocks (early Eocene) and the oldest sampled products of Himalayan erosion in the high $^{87}Sr/^{86}Sr$ Dagshai Formation deposited after 30 Ma. The range of the detrital mineral ages in the Dagshai Formation shows that the source rock was being cooled through the 350 °C blocking temperature for Ar in muscovite as early as 32 Ma.

The timing of the inflexion in the seawater Sr-isotope curve is thus consistent with the hypothesis that it results from the onset of exhumation of high $^{87}Sr/^{86}Sr$ High Himalayan Crystalline Series rocks in the Himalayas. It is of interest that the initial High Himalayan Crystalline Series rocks eroded were relatively low grade (subgarnet) with a progressive increase in metamorphic grade with continued unroofing (Najman and Garzanti, 2000). Possible equivalents to these low-grade rocks have recently been mapped by their Sm–Nd isotope systematics as an external tectonic unit within the Lesser Himalayas in Gharwal (Ahmad *et al.* 2000).

Conclusions

Himalayan erosion during the late Palaeocene to early Eocene was dominantly of Indus Tsangpo Suture Zone and Tibetan Sedimentary Series rocks. However, by Dagshai Formation times (25 Ma and possibly earlier), the High Himalaya supplied the majority of the detritus to the foreland basin, a situation which continues to the present day. This change is interpreted to reflect the first unroofing of the rocks that now form the High Himalayan Crystalline Series. Uplift of the High Himalaya to form a topographic barrier between Indus Tsangpo Suture Zone rocks and the basin explains the marked paucity of volcanic input in the Dagshai Formation compared with the Subathu formation. The proto-High Himalayan thrust sheets became the dominant source from the time of deposition of the Dagshai Formation ($<$ 30 Ma), until today. Uplift of these high $^{87}Sr/^{86}Sr$ rocks began sometime between mid-Eocene ($\approx$ 50 Ma) and $\sim$ mid-Oligocene ($\approx$ 30 Ma) epochs, possibly coincident with the timing of the start of increase in $^{87}Sr/^{86}Sr$ in the marine record at 40 Ma.

Acknowledgements

E. Laws, D. Najman and A. Skelton are thanked for field assistance, Laxsman Dass and Chamel Singh for driving. This work was supported by a Royal Society Dorothy Hodgkin Research Fellowship and Royal Society Research Grant awarded to the first author. Cambridge University supported isotopic analyses.

References

Ahmad, T., Harris, N., Bickle, M., Chapman, H., Bunbury, J. and Prince, C., 2000. Isotopic constraints on the structural relationships between the Lesser Himalayan Series and the High Himalayan Crystaline Series, Garhwal Himalaya. *Bull. Geol. Soc. Am.*, **112**, 467–477.

Ayres, M. and Harris, N., 1997. REE fractionation and Nd-isotope disequilibrium during crustal anatexis: constraints from Himalayan leucogranites. *Chem. Geol.*, **139**, 249–269.

Bhatia, S.B., 1982. Facies, fauna and flora in the lower Tertiary formations of Northwestern Himalayas: a synthesis. *Spec. Publ. Palaeont. Soc. India*, **1**, 8–20.

Bickle, M.J., Wickham, S.M., Chapman, H.J. and Taylor, H.P., 1988. A strontium, neodymium and oxygen isotope study of hydrothermal metamorphism and crustal anatexis in the Trois Seigneurs massif, Pyrenees, France. *Contr. Miner. Petrol.*, **100**, 399–417.

Bouquillon, A., France-Lanord, C., Michard, A. and Tiercelin, J., 1990. Sedimentology and isotopic chemistry of the Bengal Fan sediments: the denudation of the Himalaya. *Proc. Ocean drill. Progr., Sci. Results*, **116**, 43–58.

Burbank, D.W., Beck, R.A. and Mulder, T., 1996. The Himalayan foreland basin. In: *The Tectonic Evolution of Asia*. (A. Yin and T.M. Harrison, eds), pp. 149–188. Cambridge University Press, Cambridge.

Critelli, S. and Garzanti, E., 1994. Provenance of the Lower Tertiary Murree redbeds (Hazara-Kashmir Syntaxis, Pakistan) and initial rising of the Himalayas. *Sediment. Geol.*, **89**, 265–284.

Deniel, C., Vidal, P. and Le Fort, P., 1986. The Himalayan leucogranites and their probable parent material: the Tibet slab gneisses. *C. R. Acad. Sci. Paris*, **303**, 57–62.

Deniel, C., Vidal, P., Fernandez, A. and Le Fort, P., 1987. Isotopic study of the Manaslu granite (Himalaya, Nepal): inferances of the age and source of Himalayan leucogranites. *Contr. Miner. Petrol.*, **96**, 78–92.

Derry, L.A. and France-Lanord, C., 1996. Neogene Himalayan weathering history and river $^{87}Sr/^{86}Sr$ impact on the marine Sr record. *Earth Planet. Sci. Lett.*, **142**, 59–74.

Dietrich, V. and Gansser, A., 1981. The leucogranites of the Bhutan Himalaya. *Schweiz. Miner. Petrol. Mitt.*, **61**, 177–202.

England, P. and McKenzie, D., 1982. A thin viscous sheet model for continental deformation. *Geophys. J. R. astr. Soc.*, **70**, 295–321.

Ferrara, G., Lombardo, B. and Tonarini, S., 1983. Rb/Sr geochronology of granites and gneisses from the mt Everest region of the Nepal Himalayas. *Geol. Rndsch.*, **72**, 119–136.

Ferrara, G., Lombardo, B., Tonari, S. and Turi, B., 1991. Sr, Nd and O isotopic characterisation of the Gophu La and Gumberanjun leucogranites (High Himalaya). *Schweiz. Miner. Petrol. Mitt.*, **71**, 31–51.

Fiestmantel, O., 1882. Note on the remains of palm leaves from Tertiary Muree and Kasauli beds in India. *Records Geol. Surv. India*, **15**, 51–53.

France-Lanord, C. and Le Fort, P., 1988. Crustal melting and granite genesis during the Himalayan collision orogenesis. *Trans. R. Soc. Edinb. (Earth Sci.)*, **79**, 183–195.

France-Lanord, C., Derry, L. and Michard, A., 1993. Evolution of the Himalaya since Miocene time: isotopic and sedimentological evidence from the Bengal fan. In: *Himalayan Tectonics* (P.J. Treloar and M.P. Searle, eds), Spec. Publ. Geol. Soc. Lond., **74**, 603–621.

Friend, P.F., 1998. General form and age of the denudation system of the Himalaya. *GFF*, **120**, 231–236.

Galy, A. and France-Lanord, C., 1999. Weathering processes in the Ganges-Brahmaputra basin and the river alkalinity budget. *Chem. Geol.*, **159**, 31–60.

Galy, A., France-Lanord, C. and Derry, L.A., 1996. The late Oligocene early Miocene Himalayan belt: constraints deduced from isotopic compositions of early Miocene turbidites in the Bengal fan. *Tectonophysics*, **260**, 109–118.

Gansser, A., 1964. *Geology of the Himalyas*. Interscience, London, 289pp.

Garzanti, E. and Van Haver, T., 1988. The Indus clastics: forearc basin sedimentation in the Ladakh Himalaya (India). *Sediment. Geol.*, **59**, 237–249.

Harris, N.B.W., Bickle, M.J., Chapman, H.J., Fairchild, I. and Bunbury, J., 1998. The significance of Himalayan rivers for silicate weathering rates: evidence from the Bhoti Kosi tributary. *Chem. Geol.*, **144**, 205–220.

Harrison, T.M., Ryerson, F.J., Le Fort, P., Yin, A., Lovera, O.M. and Catlos, E.J., 1997. A late Miocene-Pliocene origin for the central Himalayan inverted metamorphism. *Earth Planet. Sci. Lett.*, **146**, E1–E7.

Harrison, T.M., Grove, M., McKeegan, K.D., Coath, C.D., Lovera, O.M. and Le Fort, P., 1999. Origin and episodic emplacment of the Manaslu intrusive complex, central Himalaya. *J. Petrol.*, **40**, 3–19.

Hodell, D.A., Mead, G.A. and Mueller, P.A., 1990. Variation in the strontium isotope composition of sea water (8 Ma to present): Implications for chemical weathering rates and dissolved fluxes to the oceans. *Chem. Geol. (Isotop. Geosci. Sect.)*, **80**, 291–307.

Hodges, K.V. and Silverberg, D.S., 1988. Thermal evolution of the Greater himalaya, Garhwal. India. *Tectonics*, **7**, 583–600.

Hodges, K.V., Hames, W.E., Olszewski, W., Burchfiel, B.C., Royden, L.H. and Chern, Z., 1994. Thermobarometric and $^{40}Ar/^{39}Ar$ geochronologic constraints on Eo Himalayan metamorphism in the Dinggye area, southern Tibet. *Contr. Miner. Petrol.*, **117**, 151–163.

Hodges, K.V., Parrish, R.R. and Searle, M.P., 1996. Tectonic evolution of the central Annapurna Range. *Tectonics*, **15**, 1264–1291.

Honegger, K., Dietrich, V., Frank, W., Gansser, A., Thoni, M. and Trommsdorf, V., 1982. Magmatism and metamorphism in the Ladakh himalaya (the Indus Tsangpo Suture Zone). *Earth Planet. Sci. Lett.*, **60**, 253–292.

Houseman, G. and England, P., 1993. Crustal thickening versus lateral expulsion in the Indian-Asian continetal collision. *J. Geophys. Res.*, **98**, 12233–12249.

Hubbard, M.S. and Harrison, T.M., 1989. $^{40}Ar/^{39}Ar$ age constraints on deformation and metamorphism on the main Central Thrust Zone and Tibetan Slab, Eastern Nepal Himalaya. *Tectonics*, **8**, 865–880.

Inger, S. and Harris, N.B.W., 1992. Tectonothermal evolution of the High Himalayan Crystalline sequence, Langtang Valley, Northern Nepal. *J. Metamorph. Geol.*, **10**, 439–452.

Inger, S. and Harris, N.B.W., 1993. Geochemical constraints on leucogranite magmatism in the Langtang Valley, Nepal Himalaya. *J. Petrol.*, **34**, 345–368.

Johnson, N.M., Stix, J., Tauxe, L., Cerveny, P.F. and Tahirkheli, R.A.K., 1985. Palaeomagnetic chronology, fluvial processes and tectonic implications of the Siwalik deposits near Chinji Village. Pakistan. *J. Geol.*, **93**, 27–40.

Kai, K., 1981. Rb-Sr geochronology of the rocks of the Himalayas, Eastern Nepal, Part 2, The age and origin of the granite on the Higher Himalayas. *Mem. Fac. Sci. Kyoto Univ. Geol. Miner. Ser.*, **157**, 149–157.

Le Fort, P., 1996. Evolution of the Himalaya. In: *The Tectonic Evolution of Asia* (A. Yin and T.M. Harrison, eds), pp. 95–109. Cambridge University Press, Cambridge.

Le Fort, P., Cuney, M., Deniel, C. *et al.*, 1987. Crustal generation of the Himalayan leucogranites. *Tectonophysics*, **134**, 39–57.

Lightfoot, P.C., Hawkesworth, C.J., Devey, C.W., Rogers, N.W. and Van Calsteren, P.W.C., 1990. Source and differentiation of Deccan trap lavas: Implications of geochemical and mineral chemical variations. *J. Petrol.*, **31**, 1165–1200.

Massey, J.A., 1994. Fluid circulation and fault controlled magmatism in the Central Himalayas. Unpubl. doctoral dissertation, Open University, UK, 399pp.

Mathur, N.S., 1980. Biostratigrphic aspects of the Subathu Formation, Kuman Himalaya. *Recent Res. Geol.*, **5**, 96–112.

Meigs, A.J., Burbank, D.W. and Beck, R.A., 1995. Middle-late Miocene (10 Ma) formation of the Main Boundary Thrust in the Western Himalaya. *Geology*, **23**, 423–426.

Najman, Y. and Garzanti, E., 2000. Reconstructing early Himalayan tectonic evolution and paleogeography from tertiary foreland basin sediments, Northern India. *Bull. Geol. Soc. Am.*, **112**, 435–449.

Najman, Y.M.R., 1995. Evolution of the early Himalayan foreland basin in N.W. India and its relationship to Himalayan orogenesis. Unpubl. doctoral dissertation, University of Edinburgh, 374pp.

Najman, Y.M.R., Clift, P., Johnson, M.R.W. and Robertson, A.H.F., 1993. Early stages of foreland basin evolution in the Lesser Himalaya, N. India. In:

Himalayan Tectonics (P.J. Treloar and M.P. Searle, eds). *Spec. Publ. Geol. Soc. Lond.*, **74**, 541–558.

Najman, Y.M.R., Enkin, R.J., Johnson, M.R.W., Robertson, A.H.F. and Baker, J., 1994. Paleomagnetic dating of the earliest continental Himalayan foredeep sediments: implications for Himalayan evolution. *Earth Planet. Sci. Lett.*, **128**, 713–718.

Najman, Y.M.R., Pringle, M.S., Johnson, M.R.W., Robertson, A.H.F. and Wijbrans, J.R., 1997. Laser $^{40}Ar/^{39}Ar$ dating of single detrital muscovite grains from early foreland basin sediments in India: Implications for early Himalayan evolution. *Geology*, **25**, 535–538.

Najman, Y.M.R., Johnson, C., Bickle, M.J. and Chapman, H.J., 1999. Insights into Himalayan exhumation, foredeep evolution, and the relationship between the erosion of the orogen and the marine Sr record from detrital zircon fission track analyses and whole-rock Sr isotope analyses of the Indian foredeep sediments (Abstract). *Terra Nostra*, **99**, 106–108.

Parrish, R.P. and Hodges, K.V., 1996. Isotopic constraints on the age and provenance of the Lesser and Greater Himalayan sequences. *Bull. Geol. Soc. Am.*, **108**, 904–911.

Peucat, J.J., Vidal, P., Bernard-Griffiths, J. and Condie, K.C., 1989. Sr, Nd and Pb isotopic systematics in the Archaean low-grade to high-grade transition zone of southern India–syn-accretion vs post-accretion granulites. *J. Geol.*, **97**, 537–549.

Raymo, M.E., 1991. Geochemical evidence supporting T.C. Chamberlin's theory of glaciation. *Geology*, **19**, 344–347.

Richter, F.M., Rowley, D.B. and DePaolo, D.J., 1992. Sr isotope evolution of seawater: the role of tectonics. *Earth Planet. Sci. Lett.*, **109**, 11–23.

Robertson, A.H.F. and Degnan, P.J., 1993. Sedimentology and tectonic implications of the Lamayuru Complex: deep water facies of the Indian Passive margin. In: *Himalayan Tectonics* (P.J. Treloar and M.P. Searle, eds). *Spec. Publ. Geol. Soc. Lond.*, **74**, 299–322.

Rowley, D.B., 1996. Age of initiation of collision between India and Asia: a review of the stratigraphic data. *Earth Planet. Sci. Lett.*, **145**, 1–13.

Scaillet, B., France-Lanord, C. and Le Fort, P., 1990. Badrinath-Gangotri plutons (Garhwal, India): petrological and geochemical evidence for fractionation processes in a high Himalayan leucogranite. *J. Volcanol. Geotherm. Res.*, **44**, 163–188.

Searle, M.P. and Fryer, B.J., 1986. Garnet, tourmaline and muscovite-bearing leucogranites, gneisses and migmatites of the Higher Himalayas from Zanskar, Kulu, Lahoul and Kashmir. In: *Collision Tectonics* (M.P. Coward and A.C. Ries, eds). *Spec. Publ. Geol. Soc. Lond.*, **19**, 185–201.

Searle, M., Corfield, R.I., Stephenson, B. and McCarron, J., 1997a. Structure of the North Indian continental margin in the Ladakh-Zanskar Himalayas: implications for the timing of obduction of the Spontang ophiolite, India-Asia collision and deformation events in the Himalaya. *Geol. Mag.*, **134**, 297–316.

Searle, M.P., Parrish, R.P., Hodges, K.V., Hurford, A., Ayres, M.W. and Whitehouse, M.J., 1997b. Shisha Pangma leucogranite, South Tibetan Himalaya: field relations, geochemistry, age, origin and emplacement. *J. Geol.*, **105**, 295–317.

Searle, M.P., Noble, S.R., Hurford, A.J. and Rec, D.C., 1999. Age of crustal melting, emplacement and exhumation history of the Shivling leucogranite, Garhwal Himalaya. *Geol. Mag.*, **136**, 513–525.

Singh, S.K., Trivedi, J.R., Pande, K., Ramesh, R. and Krishnaswami, S., 1998. Chemical and strontium, oxygen, and carbon isotopic compositions of carbonates from the Lesser Himalaya: Implications to the strontium isotope composition of the source waters of the Ganga, Ghaghara, and the Indus rivers. *Geochim. Cosmochim. Acta.*, **62**, 743–755.

Stern, C.R., Kligfield, R., Schelling, D. *et al.*, 1989. The Bhagirathi leucogranite of the high Himalaya (Garhwal India); age, petrogenesis and tectonic implications. *Spec. Pap. Geol. Soc. Am.*, **232**, 33–45.

Tapponnier, P., Peltzer, G., Le Dain, A.Y. and Armijo, R., 1982. Propagating extrusion tectonics in Asia: new insights from simple experiments with plasticine. *Geology*, **10**, 611–616.

Taylor, S.R. and McLennan, S.M., 1985. *The continental crust. Its Composition and Evolution.* Blackwell Scientific Publications. Oxford, 312pp.

Trivedi, J.R., Gopalan, K. and Valdiya, K.S., 1984. Rb-Sr ages of granitic rocks within the Lesser Himalayan nappes, Kumaun. India. *J. Geol. Soc. India*, **25**, 641–654.

Valdiya, K.S., 1980. *Geology of Kumaun Lesser Himalaya.* Wadia Insitute of Himalayan Geology, Dehra Dun, 291pp.

Vance, D. and Harris, N., 1999. Timing of prograde metamorphism in the Zanskar Himalaya. *Geology*, **27**, 395–398.

Vidal, P., Cocherie, A. and Le Fort, P., 1982. Geochemical investigations of the origin of the Manaslu leucogranite (Himalaya, Nepal). *Geochim. Cosmochim. Acta.*, **46**, 2279–2292.

Received 3 November 1999; revised version accepted 4 May 2000

